

Analytical Methods

Accepted Manuscript



This is an *Accepted Manuscript*, which has been through the Royal Society of Chemistry peer review process and has been accepted for publication.

Accepted Manuscripts are published online shortly after acceptance, before technical editing, formatting and proof reading. Using this free service, authors can make their results available to the community, in citable form, before we publish the edited article. We will replace this *Accepted Manuscript* with the edited and formatted *Advance Article* as soon as it is available.

You can find more information about *Accepted Manuscripts* in the [Information for Authors](#).

Please note that technical editing may introduce minor changes to the text and/or graphics, which may alter content. The journal's standard [Terms & Conditions](#) and the [Ethical guidelines](#) still apply. In no event shall the Royal Society of Chemistry be held responsible for any errors or omissions in this *Accepted Manuscript* or any consequences arising from the use of any information it contains.

1
2
3
4
5
6
7
8
9
10
11
12
13
14
15
16
17
18
19
20
21
22
23
24
25
26
27
28
29
30
31
32
33
34
35
36
37
38
39
40
41
42
43
44
45
46
47
48
49
50
51
52
53
54
55
56
57
58
59
60

**Fluorescent detection of Mucin 1 protein based on aptamer
functionalized biocompatible carbon dots and graphene oxide**

YanJun Ding^{1*}, Jiang Ling¹, Hao Wang¹, Jiang Zou¹, Kangkai Wang¹, Xianzhong

Xiao¹, Minghui Yang^{2*}

1 Department of Pathophysiology, Xiangya School of Medicine, Central South University, Changsha 410008, P.R. China.

2 Department of Chemistry and Chemical Engineering, Central South University, Changsha 410008, P.R. China.

Correspondence to: YanJun Ding

email: dingyanjun@csu.edu.cn

Phone: (86) 731 82355022

Correspondence to: Minghui Yang

email: yangminghui@csu.edu.cn

Phone: (86) 731 88836356

1
2
3
4 ABSTRACT: An ultrasensitive aptasensor for detection of Mucin 1 (MUC1) protein
5
6 based on fluorescence resonance energy transfer (FRET) between carbon dots (CDs)
7
8 and graphene oxide (GO) was reported. Taking advantage of strong fluorescence and
9
10 good biocompatibility of CDs, the MUC1 aptamer was covalently conjugated to CDs
11
12 (aptamer-CDs) to capture MUC1 protein through high affinity interaction between
13
14 aptamer and MUC1 protein. The FRET process between aptamer-CDs and GO is
15
16 easily achieved due to their efficient self-assembly through specific π - π interaction, in
17
18 which the fluorescence of CDs was efficiently quenched. In the presence of target
19
20 MUC1 protein, the association constant between aptamer-CDs and MUC1 is bigger
21
22 than aptamer-CDs and GO, leading to the release of the aptamer-CDs from GO, and
23
24 resulted in the recovery of CDs fluorescence. This was shown to detect MUC1 protein
25
26 specifically and sensitively in a linear range from 20.0 to 804.0 nM with a detection
27
28 limit of 17.1 nM. The developed aptasensor is highly biocompatible and nontoxic,
29
30 which can be easily modified for the detection of other protein biomarker.
31
32
33
34
35
36
37
38
39
40

41 **Keywords:** aptasensor, fluorescence resonance energy transfer, carbon dots, graphene
42
43
44 oxide, Mucin 1
45
46
47
48
49
50
51
52
53
54
55
56
57
58
59
60

1. Introduction

Biomolecular detection has shown more and more critical application in early diagnostics and treatment of diseases, which has promoted intensive interest in the development of trustworthy, simple and low-cost biosensors for proteins, nucleic acids and other biomolecules.^{1,2} Aptamer, a kind of single-stranded oligonucleic acids or peptide molecules, shows high affinity to specific targets like proteins, peptides, organic molecules, metal ions, as well as cells, and thus is well recognized as a useful tool for binding target biomolecules.^{3,4} Aptamer-functionalized nanomaterials integrated the advantages of both aptamer and nanomaterials, and displayed great potential applications in the construction of biosensors,⁵ biosystem imaging⁶ and targeted in vivo drug delivery.⁷ Recently, novel nanomaterials have attracted great attention and have been intensively studied in biological analysis and detection. Due to their quantum effects proceeding from the large surface area-to-volume ratio, nanomaterials including Au nanoparticles, semiconductor QDs and carbon-based nanomaterials possess unique optical, electrical, catalytic and magnetic properties, and thus are widely applied to the detection of biological species.⁸⁻¹⁰

Fluorescence resonance energy transfer (FRET) from an excited state of a donor to a proximal ground state acceptor, is widely used in biological analysis.^{11,12} Excellent donor-acceptor pairs and good biocompatibility of donor-acceptor pairs are two significant factors to improve the efficiency of FRET and the resulting analytical performance. However, current-used fluorescent probes including organic dyes and inorganic semiconductor quantum dots have their own drawbacks including poor

1
2
3
4 photostability, easy photobleaching, small Stokes shifts, short lifetimes and significant
5
6 toxicity even at relatively low concentrations,^{13, 14} which may prove prohibitive to
7
8 patient studies. Therefore, the search for better alternatives has continued. Carbon is
9
10 hardly considered as an intrinsically toxic element. Of particular interest and
11
12 significance was the recent finding that small carbon nanoparticles could be
13
14 surface-passivated by organic or biomolecules to become strongly fluorescent.^{15, 16}
15
16 These fluorescent carbon nanoparticles named “carbon dots” were found to be
17
18 physicochemically and photochemically stable and nonblinking. Carbon dots (CDs)
19
20 are quasi-spherical nanoparticles with good biocompatibility and tunable surface
21
22 functionalities. These superior properties afforded the use of CDs in broad fields such
23
24 as bio-imaging¹⁷ and sensing.^{18, 19}
25
26
27
28
29
30

31 Graphene oxide (GO) possesses oxygen containing functional groups²⁰ and an
32
33 unique microstructure composed of sp^2 carbons surrounded by sp^3 carbons, which
34
35 give it an excellent aqueous solubility and hence their potential fluorescence
36
37 quenching ability²¹. Recently, it has been employed as a good energy acceptor that
38
39 could quench the fluorescence of semiconductor quantum dots, metal nanoclusters
40
41 and organic dye and so on. Wei and co-workers¹² constructed a GO FRET aptasensor
42
43 for MCF-7 breast cancer cells detection based on the dye -labeled aptamer assembled
44
45 on GO.
46
47
48
49
50

51 In this paper, CDs and GO were designed respectively as the energy donor and
52
53 acceptor for the FRET system. This system used Mucin 1 (MUC1) aptamer labeled
54
55 CDs (aptamer-CDs) as a probe. MUC1 is a tumor marker encoded by the MUC1 gene
56
57
58
59
60

1
2
3
4 in humans.²² It is often overexpressed on the surface of cancer cells like breast,
5
6 ovarian, lung and pancreatic cancers.²³ A 25-base oligonucleotide (aptamer) has
7
8 specific binding properties for MUC1 peptide.²⁴ The fluorescence of the aptamer-CDs
9
10 could be quenched efficiently by GO due to the FRET. As shown in Scheme 1, high
11
12 quenching efficiency of fluorescence occurred when the aptamer-CDs was bound to
13
14 GO, due to decrease in distance between GO and CDs. Upon recognition of the
15
16 aptamer to the target MUC1 protein, the fluorescence increased significantly since the
17
18 formation of the aptamer–MUC1 complex led to the release of aptamer-CDs from the
19
20 surface of GO, which increased the distance between GO and CDs, hindered the
21
22 energy transfer, and recovered the fluorescence of CDs. This system was
23
24 demonstrated to possess high sensitivity and displayed promising applications in
25
26 biomolecule detection.
27
28
29
30
31
32

33 34 35 **2. Experimental**

36 37 38 2.1. Materials and reagents

39
40 1-Ethyl-3-(3-dimethylaminopropyl) carbodiimide hydrochloride (EDC),
41
42 N-hydroxysuccinimide (NHS), MUC1 protein and IgG were purchased from Abcam
43
44 Company (Cambridge, UK). The MUC1 aptamer, complementary strand and a
45
46 three-base mismatched strand DNA (mDNA) were synthesized by Sangon Biological
47
48 Engineering Technology & Co. Ltd. (Shanghai, China) and purified using
49
50 high-performance liquid chromatography. Their sequences were:
51
52

53
54
55 MUC1 aptamer: 5'-NH₂-GCAGTTGATCCTTTGGATACCCTGG-HPO₄-3'

56
57
58 Complementary strand (cDNA): 5'-CCAGGGTATCCAAAGGATCAACTGC-3'
59
60

1
2
3
4 A three-base mismatched strand (mDNA):

5
6 5'-CCAGGGTATGCGACGGATCAACTGC-3'
7

8
9 Ethylenediamine, citric acid, nitric acid and sodium carbonate (Na_2CO_3) were
10
11 obtained from Sinopharm Chemical Reagents Co., Ltd. Phosphate buffer solution
12
13 (PBS) was prepared using 0.01M Na_2HPO_4 and 0.01M KH_2PO_4 . All other chemicals
14
15 were of analytical grade and used as received.
16
17

18
19 Fluorescence spectra were measured by an FL-4600 spectrometer (Hitachi, Japan).
20
21 UV-Visible absorption spectra were collected on a Shimadzu UV-2450
22
23 spectrophotometer. Transmission electron microscopy (TEM) images were obtained
24
25 from T20 FEI TECNAI G2 (America, FEI). Samples were prepared by dropping
26
27 aqueous suspensions of aptamer-CDs, GO and aptamer-CDs/GO onto Cu TEM grids
28
29 coated with a holey amorphous carbon film and following solvent evaporation in a
30
31 dust protected atmosphere.
32
33

34 35 36 2.2. Synthesis of carbon dots (CDs)

37
38
39 CDs were synthesized according to the reference.¹⁹ 1.05 g Citric acid and 335 μL
40
41 ethylenediamine were dissolved in 10 mL deionized water. Then the solution was
42
43 transferred to a Teflon-lined autoclave (30 mL) and heated at 250 °C for 5 h.
44
45 Subsequently, the crude CDs suspension was mixed with concentrated nitric acid and
46
47 heated at reflux for 12 h to obtain abundant carboxyl groups on the surface of CDs.
48
49 After cooling to room temperature, the obtained solution was first neutralized by
50
51 Na_2CO_3 solution. Then, the carbogenic nanoparticles obtained above were dialyzed
52
53 against Milli-Q water for 3 days to remove all salts. The suspension appeared
54
55
56
57
58
59
60

1
2
3 homogeneous light yellow and was finally stored at 4 °C in a refrigerator. The
4
5
6 nanosized carbon dots were of 5 nm as estimated from TEM images.
7

8 9 2.3. Preparation of aptamer–CDs probe

10
11 The 3'-phosphate of the MUC1 aptamer was covalently combined to the carboxyl
12
13 group of CDs as in previous reports.²⁵ Generally, the 3'- phosphate group of the
14
15 MUC1 aptamer was first activated by adding 200 mL of a 0.10 M imidazole solution
16
17 (pH 6.8) to 2 OD (optical density, 1 OD at 260 nm \approx 4.31 nM ssDNA) of the aptamer
18
19 for 30 min. Simultaneously, 1-ethyl-3-(3-dimethylamino propyl)-carbodiimide (EDC)
20
21 (120 μ L, 0.4 M) and N-hydroxysulfosuccinimide sodium salt (NHS) (120 μ L, 0.1 M)
22
23 were added to the above CDs solution to activate the surface carboxylic group for 30
24
25 min at room temperature with continuous stirring. Subsequently, the activated CDs
26
27 and aptamer (15.0 μ L, 200.0 μ M) were mixed together and allowed to react overnight
28
29 at room temperature with continuous stirring. The aptamer–CDs bioconjugates were
30
31 obtained by centrifugation and washing with PBS buffer three times to remove the
32
33 free nonconjugated complex and by-products.
34
35
36
37
38
39

40 41 2.4. Synthesis of graphene oxide (GO).

42
43 GO was synthesized by natural graphite oxidation using a modified Hummer's
44
45 method. Generally, 12 mL concentrated H₂SO₄ was put into a round bottom flask and
46
47 cooled to 4 °C by using an ice bath. Then, added 0.4 g graphite powder and 0.2 g
48
49 NaNO₃ under intense stirring for 30 minutes, followed by the addition of 1.2 g
50
51 KMnO₄ in many times in 2 h. During these processes, the temperature of the mixture
52
53 was maintained at 4 °C. Then it was heated to 35 °C by using oil bath for 4 h. After
54
55
56
57
58
59
60

1
2
3
4 that, the mixture was diluted with 40 mL H₂O slowly and the temperature was
5
6 increased to 90 °C. Then 4 mL 30 % H₂O₂ was added drop by drop after cooling the
7
8 above mixture for about 0.5~ 1 h. After being cooling down to room temperature, the
9
10 mixture was centrifuged and washed with 5 % HCl five times, and then with
11
12 deionized water to neutral, and finally dried in air to obtain the GO.
13
14

15 16 2.5. Determination of MUC1 protein 17

18
19 The quenching effect of GO on fluorescence of aptamer-CDs was carried out as
20
21 follows: 100 μL of aptamer-CDs (45.0 μg mL⁻¹) suspension in PBS was prepared at
22
23 first, then, a series of 20 μL GO solutions with various concentrations were added and
24
25 the final mixture solution was diluted to 300 μL with PBS. After 30 min of
26
27 sonification and another 30 min of standing to ensure sufficient adsorption of the
28
29 aptamer-CDs on GO, the fluorescence intensities of resulting mixtures were recorded
30
31 using fluorescence spectrometer. For MUC1 protein detection, a series of 20 μL target
32
33 MUC1 protein with different concentrations was incubated with the aptamer-CDs/GO
34
35 mixture at 37 °C for 60 min. The resulted solutions were finally diluted to 300 μL
36
37 with PBS and the fluorescence intensity was measured under the optimal excitation
38
39 wavelength of 390 nm. The fluorescence dependent on time of quenching and
40
41 recovery were conducted by monitoring fluorescence intensity at different incubation
42
43 times.
44
45
46
47
48
49
50
51
52
53

54 3. Results and discussion 55

56 3.1. Conjugation of aptamer with carbon dots (CDs) 57 58 59 60

1
2
3
4 After activation of the 3' phosphate group with imidazole, the aptamer was reacted
5
6 with the carboxyl group on the surface of CDs in the presence of EDC and NHS to
7
8 produce the aptamer-CDs conjugates. The conjugation of the CDs and aptamer was
9
10 illustrated by UV-vis absorption spectra. Fig.1 shows the UV-vis absorption spectra of
11
12 the CDs, aptamer, and aptamer - CDs in 0.01 M pH 7.4 PBS. The UV-vis absorption
13
14 spectra of CDs shows a maximum adsorption peaks at ~340 nm which corresponds to
15
16 $\pi-\pi^*$ transition of C=C bonds and respectively to $n-\pi^*$ transitions of C=O bonds (Fig.
17
18 1a). A characteristic absorption peak at ~260 nm is observed for the MUC1 aptamer
19
20 (Fig. 1c). The aptamer-CDs maintained the characteristic absorption peaks of both the
21
22 MUC1 aptamer and the CDs, indicating the successful labeling of the aptamer with
23
24 CDs (Fig. 1b).

3.2. Characterization of CDs, aptamer-CDs, graphene oxide (GO) and aptamer-CDs/GO

35
36 The successful synthesis of GO and CDs are demonstrated by FT-IR spectra (Fig.2).
37
38 The FT-IR spectrum of the as-synthesized GO display the characteristic vibrations
39
40 that was reported in previous work,²⁶ including a broad and intense peak of an O-H
41
42 group at 3443 cm^{-1} , an OH deformation peak at 1387 cm^{-1} , a C-O stretching peak at
43
44 1094 cm^{-1} , and a peak attributed to the vibrations of unoxidized graphitic skeletal
45
46 domains and the adsorbed water molecules at 1631 cm^{-1} (Fig.2. curve GO). Also, as
47
48 can be seen from the curve CDs in Fig.2, The peaks at about 1650 cm^{-1} and 1390 cm^{-1}
49
50 indicate the existence of COO^- of the as-synthesized CDs, while the peak at 3434
51
52 cm^{-1} corresponds to the OH stretching mode.
53
54
55
56
57
58
59
60

1
2
3
4 The representative TEM images and the size distribution plots of CDs,
5
6 aptamer-CDs, GO and aptamer-CDs/GO are shown in Fig.3. As can be seen from
7
8 Figure, the size of CDs and GO are quite uniform with diameters of about 5 nm (Fig.
9
10 3a, Fig. 3c), and the size of aptamer-CDs conjugates is about 30 nm (Fig. 3b).
11
12 Compared with Fig.3b and Fig.3c, however, a clear evolution on the microstructure
13
14 can be observed for the aptamer-CDs/GO mixture (Fig.3d), in which the diameter and
15
16 morphology drastically changed and the particle size distribution become broad. It is
17
18 demonstrated that aptamer-CDs conjugates successfully assembled with GO particles.
19
20
21
22

23 3.3. Detection of MUC1 protein with FRET

24
25
26 CDs possess good biocompatibility, strong fluorescence, and thus were chosen as
27
28 the fluorophore in this aptasensor. GO with unique two-dimensional structure and
29
30 good dispersion in water after moderate oxidation was used as electron acceptor and
31
32 quenching agent in FRET. Scheme 1 displays the schematic illustration of MUC1
33
34 protein detection strategy based on FRET between MUC1 aptamer labeled CDs
35
36 (aptamer-CDs) and GO. For detection of MUC1 protein, aptamer-CDs is firstly
37
38 synthesized by conjugating aptamer and CDs via covalent coupling using EDC and
39
40 NHS. Secondly, aptamer-CDs probe is mixed with GO so that aptamer-CDs can be
41
42 adsorbed on the surface of GO through π - π stacking interaction to assemble
43
44 aptamer-CDs/GO structure. Fig.4 demonstrates the strong quenching effect of GO on
45
46 the fluorescence of aptamer-CDs and subsequent fluorescence recovery by MUC1
47
48 protein. As can be seen that the fluorescence aptamer-CDs still exhibits strong
49
50 fluorescence (Fig.4b) although it is little smaller than that of pure CDs (Fig.4a) and it
51
52
53
54
55
56
57
58
59
60

1
2
3
4 is scarcely influenced by the addition of specific target MUC1 protein in the absence
5
6 of GO (Fig.4c), however, it can be largely quenched by addition of GO without target
7
8 MUC1 protein (Fig.4d), indicating that fluorescence energy transfer between
9
10 aptamer-CDs and GO in the self-assembly process. The formation of
11
12 aptamer-CDs/GO results in nearly complete quenching of fluorescence of
13
14 aptamer-CDs probe through FRET. The quenched fluorescence can be efficiently
15
16 recovered by addition of target MUC1 protein (643 nM) (Fig.4e), which is due to the
17
18 affinity interaction between the aptamer-CDs and MUC1 protein. After addition of
19
20 MUC1 protein, the aptamer in aptamer-CDs conjugates should form the specific
21
22 configuration and MUC1 protein is captured by aptamer-CDs to produce the
23
24 MUC1/aptamer-CDs through specific base pairing. The formation of
25
26 MUC1/aptamer-CDs complexes decreased the interaction of the aptamer-CDs and GO,
27
28 and thus led to liberation and detachment of MUC1/aptamer-CDs from GO, resulting
29
30 in fluorescence recovery of CDs. In addition, GO itself exhibits no fluorescence
31
32 emission, and thus make no contribution to whole fluorescence intensity of each
33
34 sample measured.
35
36
37
38
39
40
41
42
43

44 In order to develop this analytical method based on FRET between aptamer-CDs
45
46 and GO, optimal conditions including concentration of added GO, incubation time of
47
48 fluorescence quenching and recovery were studied. Fig.5A shows the quenching
49
50 effect with various concentrations of GO. The fluorescence gradually decreases with
51
52 the increasing concentration of GO, and remains stable at $120 \mu\text{g mL}^{-1}$ GO, when
53
54 almost 95 % of the initial fluorescence is quenched. Further increase the GO
55
56
57
58
59
60

1
2
3
4 concentration leads to fluorescence intensity unchanged. Thus, $120 \mu\text{g mL}^{-1}$ was
5
6 chosen as the optimal concentration of GO. Additionally, the quenching effect with
7
8 GO and recovery efficiency with MUC1 protein as a function of incubation time are
9
10 displayed in Fig.5B. One can note that the fluorescence is gradually quenched with
11
12 time and remains nearly constant after 60 minutes in the absence of MUC1 protein
13
14 (Fig.5B, curve a). The curve for fluorescence recovery by MUC1 protein (643.0 nM)
15
16 shows a rapid growth in fluorescence intensity in the first 30 min, and then keeps
17
18 nearly unchanged in fluorescence intensity after 60 min (Fig.5B, curve c). In the
19
20 presence of target MUC1 protein, the fluorescence intensity decreased in the first 30
21
22 min, however, it tended to stabilize at higher value (Fig.5B, curve b). These time
23
24 dependent experiments clearly indicated that the MUC1 protein had a better binding
25
26 affinity to aptamer than GO, and thus the resulting MUC1/aptamer-CDs complex
27
28 prevented the fluorescence of CDs from being quenched by GO. So, 60 min were
29
30 chosen for the both optimal fluorescence quenching time and recovery time in the
31
32 following determination of MUC1 protein.
33
34
35
36
37
38
39
40

41 Under the optimal conditions, the sensing performance of this FRET system was
42
43 evaluated by adding various concentrations of MUC1 protein into aptamer-CDs /GO
44
45 mixture. The fluorescence comes from MUC1/aptamer-CDs formed between
46
47 aptamer-CDs and MUC1 protein after addition of MUC1 protein into aptamer-CDs
48
49 /GO mixture solution. As illustrated in Fig. 6A, the fluorescence intensity of
50
51 MUC1/aptamer-CDs is increased gradually with increasing concentration of MUC1
52
53 protein from 20.0 to 804.0 nM because more and more amounts of
54
55
56
57
58
59
60

1
2
3
4 MUC1/aptamer-CQD formed and escaped from GO surface during this process. The
5
6 plot of fluorescence intensity as a function of MUC1 concentration is shown in Fig.6B.
7
8 The linear equation can be expressed as $y = 2.20x + 119.83$, where $R^2 = 0.972$. The limit
9
10 of detection (LOD) was estimated about 17.1 nM according to the 3σ (standard
11
12 deviation) rule, which was lower than the previously reported biosensors.¹²
13
14

15
16 The specificity of the proposed aptamer-functionalized CDs probe was further
17
18 carried out by using different DNA sequences and proteins. The comparison of results
19
20 between the perfectly complementary strand (cDNA) and three-base mismatched
21
22 strand DNA (mDNA), MUC1 protein and IgG protein were shown in Fig.7. Upon
23
24 addition of analyte, the restored fluorescence intensity for the target MUC1 protein
25
26 (643 nM) showed the highest value (1500 a.u), while the fluorescence value for the
27
28 same concentration of IgG protein was only 150 a.u. Moreover, the response of the
29
30 cDNA (643 nM) was slightly lower than that of the target MUC1 protein with a
31
32 fluorescence value of 1280, while the response of the same concentration of mDNA
33
34 (180 a.u.) and the blank control without target (50 a.u) were very slow. These results
35
36 demonstrated that the proposed aptamer-functionalized CDs probe could easily
37
38 discriminate between the perfectly complementary strand and the MUC1 protein from
39
40 the randomly mismatched strand and other protein, which indicates that the proposed
41
42 approach has high specificity for the target detection.
43
44
45
46
47
48
49
50

51 52 53 54 **4. Conclusion**

55
56 In conclusion, a novel and effective aptasensor based on FRET between CDs and
57
58
59
60

1
2
3
4 GO for MUC1 protein detection has been established. The MUC1
5
6 aptamer-functionalized CDs were prepared and has strong fluorescence, good
7
8 biocompatibility and resistance to photobleaching. FRET can be easily achieved
9
10 because of efficient self-assembly between CDs and GO. This aptasensor can
11
12 distinguish complementary nucleic acid sequences and MUC1 protein from other
13
14 biomolecules like three-base-mismatched nucleic acid sequences and IgG with high
15
16 sensitivity and good specificity. It shows a quite broad linear scope and low detection
17
18 limit of 17.1 nM for MUC1 protein. Since all the materials involved in the sensing
19
20 system are of excellent biocompatibility, it is expected that this proposed approach
21
22 would be used in vivo and in vitro, and promotes the application of carbon-based
23
24 nanomaterials in bioassays.
25
26
27
28
29
30
31
32

33 34 **Acknowledgements**

35
36 We gratefully acknowledge the support from the National Natural Science
37
38 Foundation of China (81201486), Doctoral Fund of Ministry of Education of China
39
40 (20120162120068), and the Scientific Research Foundation for the Returned Overseas
41
42 Chinese Scholars, State Education Ministry of China.
43
44
45
46
47

48 49 **References**

- 50
51 1 R. Etzioni, N. Urban, S. Ramsey, M. McIntosh, S. Schwartz, B. Reid, J. Radich, G.
52
53 Anderson, L. Hartwell, *Nat. Rev. Cancer*, 2003, 3, 243-252.
54
55
56 2 D. A. Giljohann, C. A. Mirkin, *Nature*, 2009, 462, 461-464.
57
58
59
60

- 1
2
3
4 3 L. C. Bock, L. C. Griffin, J. A. Latham, E. H. Vermaas, J. J. Toole, *Nature*, 1992,
5
6 355, 564-566.
7
8
9 4 X. Hua, Z. X Zhou, L. Yuan, S. Q. Liu, *Analytica Chimica Acta*, 2013,
10
11 788,135-140.
12
13
14 5 J. W. Liu, Z. H. Cao, Y. Lu, *Chem. Rev.*, 2009, 109, 1948-1998.
15
16
17 6 J. Li, X. Zhong, F. Cheng, J. R. Zhang, L. P. Jiang, J. J. Zhu, *Anal. Chem.*, 2012,
18
19 84, 4140-4146.
20
21
22 7 L. Yang, L. Meng, X. Zhang, Y. Chen, G. Zhu, H. Liu, X. Xiong, K. Sefah, W.
23
24 Tan, *J. Am. Chem. Soc.*, 2011, 133, 13380-13386.
25
26
27 8 X. Chen, Y. Zhou, X. Peng, J. Yoon, *Chem. Soc. Rev.*, 2010, 39, 2120-2135.
28
29
30 9 K. Zhang, H. Zhou, Q. Mei, S. Wang, G. Guan, R. Liu, J. Zhang, Z. Zhang, *J. Am.*
31
32 *Chem. Soc.*, 2011,133 , 8424-8427.
33
34
35 10 M. Han, X. Gao, J. Z. Su, S. Nie, *Nat. Biotechnol.*, 2001, 19, 631-635.
36
37
38 11 E. A. Jares-Erijman, T. M. Jovin, *Nat. Biotechnol.*, 2003, 21, 1387-1395.
39
40
41 12 W. Wei, D. F. Li, X. H. Pan, S. Q. Liu. *Analyst*, 2012, 137, 2101-2106.
42
43
44 13 R. Hardman, *Environ Health Perspect.*, 2006, 114, 165-172.
45
46
47 14 P. Lin, J. W. Chen, L. W. Chang, J. P. Wu, L. Redding, H. Chang, T. K. Yeh, C.
48
49 S. Yang, M. H. Tsai, H. J. Wang, Y. C. Kuo, R. S. Yang, *Environ. Sci. Technol.*,
50
51 2008, 42, 6264-6270.
52
53
54 15 Y. P. Sun, B. Zhou , Y. Lin, W. Wang, K. A. Fernando, P. Pathak, M. J. Meziari,
55
56 B. A. Harruff, X. Wang, H. Wang, P. G. Luo, H. Yang, M. E. Kose, B. Chen, L. M.
57
58 Veca, S. Y. Xie, *J. Am. Chem. Soc.*, 2006, 128,7756-7757.
59
60

- 1
2
3
4 16 J. Zhou, C. Booker, R. Li, X. Zhou, T. K. Sham, X. Sun, Z. Ding, *J. Am. Chem.*
5
6 *Soc.*, 2007, 129, 744-745.
7
8
9 17 L. Cao, X. Wang, M. J. Mezziani, F. S. Lu, H. F. Wang, P. J. G. Luo, Y. Lin, B. A.
10
11 Harruff, L. M. Veca, D. Murray, S. Y. Xie, Y. P. Sun, *J. Am. Chem. Soc.*, 2007, 129,
12
13 11318-11319.
14
15
16 18 Z. S. Qian, L. J. Chai, Y.Y. Huang, C. Tang, J. J Shen, J. R. Chen, H. Feng,
17
18 *Biosens. Bioelectron.*, 2015, 68, 675-680.
19
20
21 19 Y. J. Ding, W.J Kang, X. Z. Xiao, K. K. Wang, N. Wang, H. L. Zhang, M. H.
22
23 Yang, G. L. Shen, *Australian Journal of Chemistry*,
24
25 <http://dx.doi.org/10.1071/CH14554>
26
27
28
29 20 K. P. Loh, Q. Bao, G. Eda, M. Chhowalla, *Nat. Chem.*, 2010, 2, 1015-1024.
30
31
32 21 C. Chung, Y. K. Kim, D. Shin, S. R. Ryoo, B. H. Hong, D. H. Min, *Acc. Chem.*
33
34 *Res.*, 2013, 46, 2211-2224.
35
36
37 22 S. J. Gendler, C. A. Lancaster, J. Taylorpapadimitriou, T. Duhig, N. Peat, J.
38
39 Burchell, L. Pemberton, E. Lalani, D. Wilson, *J. Biol. Chem.*, 1990, 265,
40
41 15286-15293.
42
43
44 23 S. J. Gendler, *J Mammary Gland Biol. Neoplasia*, 2001, 6, 339-353.
45
46
47 24 C. S. Ferreira, C. S. Matthews, S. Missailidis, *Tumor Biol.*, 2006, 27, 289-301.
48
49
50 25 B. C. Chu, G. M. Wahl, L. E. Orgel, *Nucleic Acids Res.*, 1983, 11, 6513-6529.
51
52
53 26 H. Dong, W. Gao, F. Yan, H. Ji, H. Ju, *Anal. Chem.*, 2010, 82, 5511-5517.
54
55
56
57
58
59
60

Figure captions:

Scheme 1. Schematic illustration of detection of MUC1 protein based on fluorescence energy transfer (FRET) between aptamer-functionalized carbon dots (CDs) and graphene oxide.

Fig.1. UV-vis spectra of (a) CDs, (b) MUC1aptamer-CDs and (c) MUC1 aptamer in 0.01M pH 7.4 PBS.

Fig.2. FT-IR spectra of carbon dots (CDs) and graphene oxide (GO).

Fig.3. TEM images of (A) CDs, (B) aptamer-CDs, (C) graphene oxide and (D) mixture between graphene oxide and aptamer-CDs.

Fig.4. The quenching effect of GO on the fluorescence of aptamer-CDs and following fluorescence recovery MUC1 protein, (a) CDs, (b) aptamer-CDs, (c) aptamer-CDs + MUC1 (643.0 nM), (d) aptamer-CDs + GO ($120 \mu\text{g mL}^{-1}$), (e) aptamer-CDs + GO ($120 \mu\text{g mL}^{-1}$) + MUC1 (643.0 nM).

Fig.5. (A) The fluorescence quenching of aptamer-CDs with different GO concentrations of 0, 10, 30, 50, 80, 120, 150 $\mu\text{g mL}^{-1}$ in 0.01M PBS (pH 7.4). Each data point represents the average of the fluorescence responses of triplicate measurements. **(B)** Time dependence of the fluorescence quenching by $120 \mu\text{g mL}^{-1}$ GO without (a) and with (b) MUC1 (643.0 nM), and (c) the fluorescence recovery with 643.0 nM MUC1 protein.

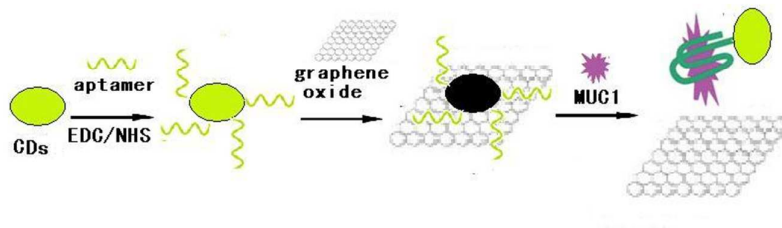
Fig.6. (A) The fluorescence recovery of aptamer-CDs/GO system after incubation with 0, 20.0, 160.0, 300.0, 352.0, 400.0, 440.0, 566.0, 643.0, 700.0, 804.0 nM MUC1.

(B) The linear relationship between the fluorescence intensity and concentration of

1
2
3
4 MUC1 protein. Each data point represents the average of the fluorescence responses
5
6 of triplicate measurements
7

8
9 **Fig.7.** Fluorescence intensity of aptamer-CDs after incubated with 643.0 nM of (a)
10
11 MUC1, (b) complementary DNA stand, (c) three-base mismatch stand (mDNA), (d)
12
13 IgG protein, (e) no target in the presence of 120 $\mu\text{g mL}^{-1}$ GO. Each data point
14
15 represents the average of the fluorescence responses of triplicate measurements
16
17
18
19
20
21
22
23
24
25
26
27
28
29
30
31
32
33
34
35
36
37
38
39
40
41
42
43
44
45
46
47
48
49
50
51
52
53
54
55
56
57
58
59
60

Scheme 1



1
2
3
4
5
6
7
8
9
10
11
12
13
14
15
16
17
18
19
20
21
22
23
24
25
26
27
28
29
30
31
32
33
34
35
36
37
38
39
40
41
42
43
44
45
46
47
48
49
50
51
52
53
54
55
56
57
58
59
60

Fig.1

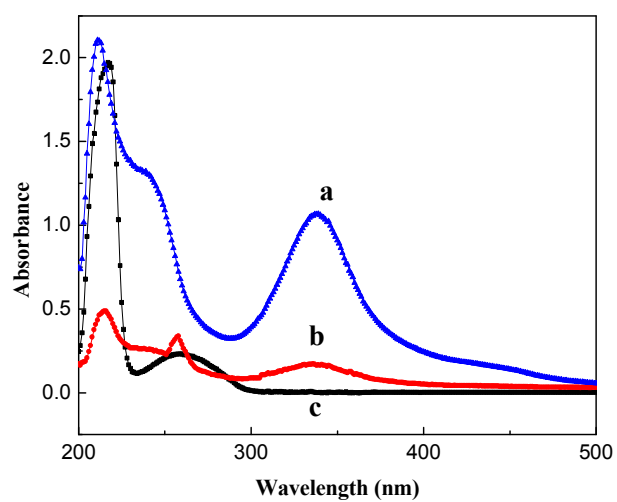
1
2
3
4
5
6
7
8
9
10
11
12
13
14
15
16
17
18
19
20
21
22
23
24
25
26
27
28
29
30
31
32
33
34
35
36
37
38
39
40
41
42
43
44
45
46
47
48
49
50
51
52
53
54
55
56
57
58
59
60

Fig.2

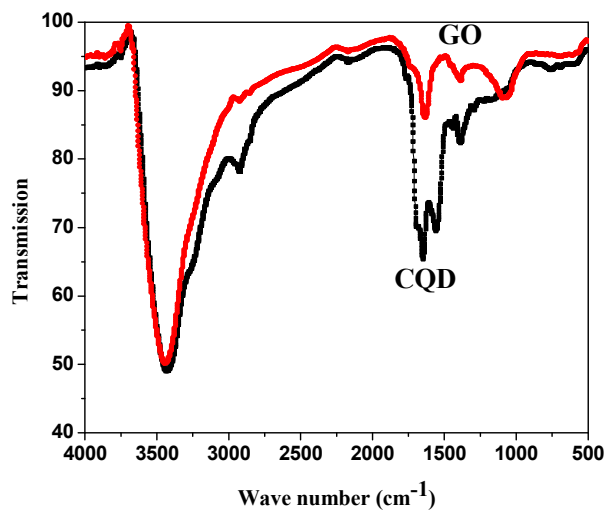
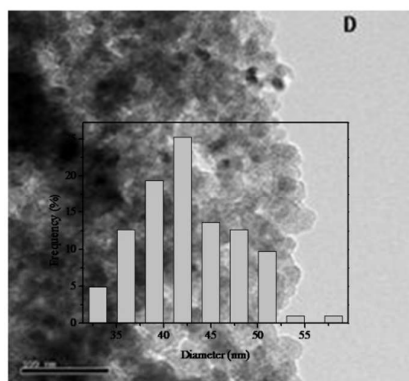
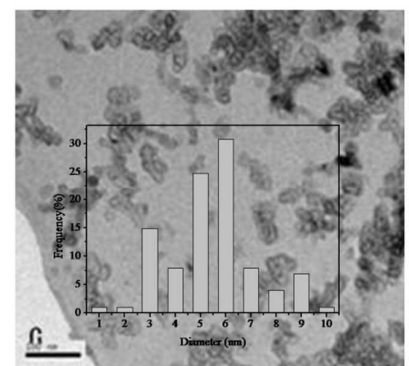
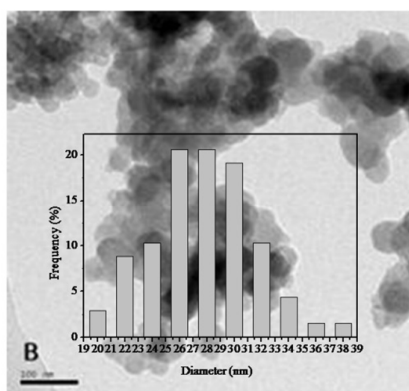
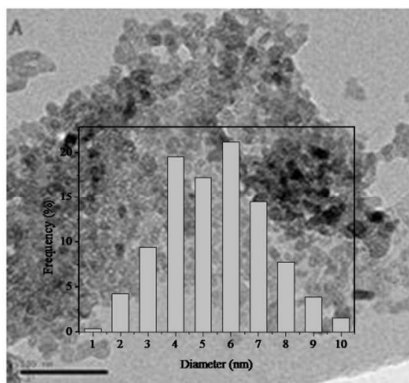
1
2
3
4
5
6
7
8
9
10
11
12
13
14
15
16
17
18
19
20
21
22
23
24
25
26
27
28
29
30
31
32
33
34
35
36
37
38
39
40
41
42
43
44
45
46
47
48
49
50
51
52
53
54
55
56
57
58
59
60

Fig.3



1
2
3
4
5
6
7
8
9
10
11
12
13
14
15
16
17
18
19
20
21
22
23
24
25
26
27
28
29
30
31
32
33
34
35
36
37
38
39
40
41
42
43
44
45
46
47
48
49
50
51
52
53
54
55
56
57
58
59
60

Fig.4

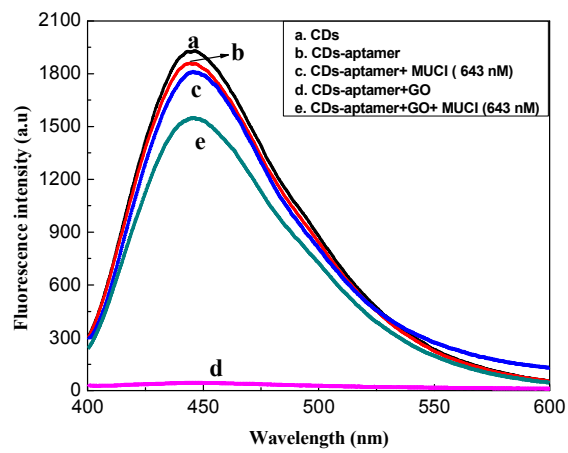
1
2
3
4
5
6
7
8
9
10
11
12
13
14
15
16
17
18
19
20
21
22
23
24
25
26
27
28
29
30
31
32
33
34
35
36
37
38
39
40
41
42
43
44
45
46
47
48
49
50
51
52
53
54
55
56
57
58
59
60

Fig.5

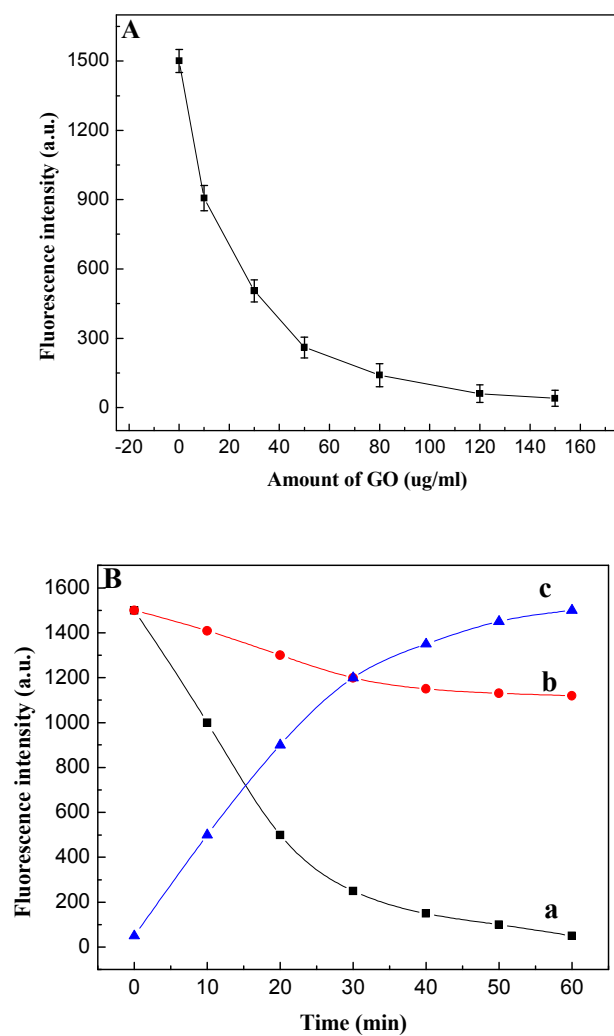
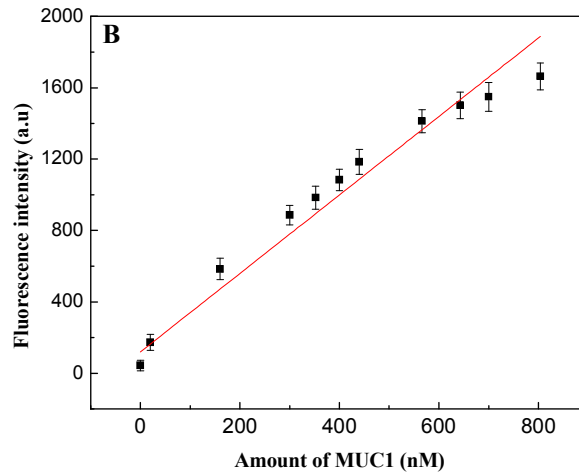
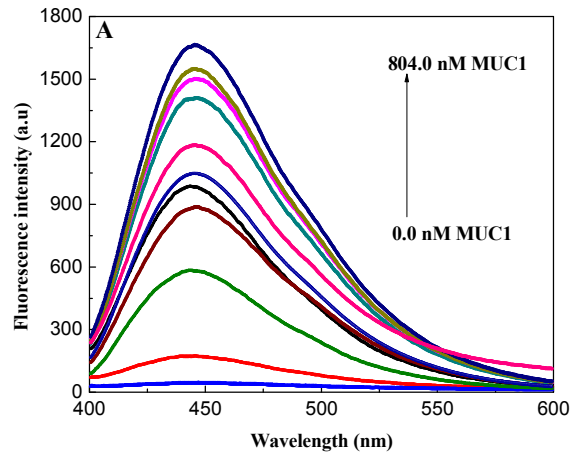
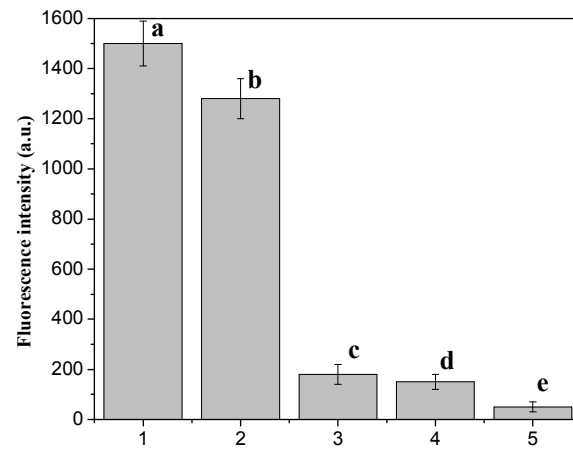


Fig.6



1
2
3
4
5
6
7
8
9
10
11
12
13
14
15
16
17
18
19
20
21
22
23
24
25
26
27
28
29
30
31
32
33
34
35
36
37
38
39
40
41
42
43
44
45
46
47
48
49
50
51
52
53
54
55
56
57
58
59
60

Fig.7.

1
2
3
4
5
6
7
8
9
10
11
12
13
14
15
16
17
18
19
20
21
22
23
24
25
26
27
28
29
30
31
32
33
34
35
36
37
38
39
40
41
42
43
44
45
46
47
48
49
50
51
52
53
54
55
56
57
58
59
60